J Shoulder Elbow Surg (2020) 29, 2632–2639

ELSEVIER

Journal of Shoulder and Elbow Surgery

www.elsevier.com/locate/ymse

Proximal-medial part in the coracoid graft demonstrates the most evident stress shielding following the Latarjet procedure: a simulation study using the 3-dimensional finite element method

Hirotaka Sano, MD, PhD[a,*], Tatsuro Komatsuda, MD, PhD[b], Hiroo Abe, MD, PhD[a], Hiroshi Ozawa, MD, PhD[c], Toshimitsu A. Yokobori Jr, PhD[d]

[a]*Division of Orthopedics, Sendai City Hospital, Sendai, Japan*
[b]*North Sendai Orthopaedic Clinic, Sendai, Japan*
[c]*Department of Orthopaedic Surgery, Tohoku Medical and Pharmaceutical University, Sendai, Japan*
[d]*Laboratory of Strength of Material and Science, Strategic Innovation and Research Center, Teikyo University, Tokyo, Japan*

Background: Although the osteolysis of the coracoid graft is frequently observed after the Latarjet procedure particularly in its proximal part, its pathomechanism is not well understood.
Methods: Three-dimensional finite element glenohumeral joint models were developed using CT-DICOM data of 10 normal shoulders. A 25% bony defect was created on the anterior glenoid rim, and the coracoid process was transferred flush with the glenoid cartilage using 2 half-threaded screws. In the hanging arm as well as in the 90° abducted positions, a compressive load (50 N) was applied to the greater tuberosity toward the center of the glenoid and a tensile force (20 N) was applied to the coracoid tip along the direction of the conjoint tendon. Next, elastic analysis was performed, and the distribution patterns of the equivalent stress as well as the maximum principal stress were compared among 4 parts (proximal/distal and medial/lateral) of the coracoid graft.
Results: Both the equivalent stress and the maximum principal stress were reduced in the proximal half of the coracoid graft. A high stress concentration was observed in the lateral aspect of the coracoid graft particularly in the 90° abducted position. The proximal-medial part demonstrated the lowest equivalent stress as well as the maximum principal stress for both arm positions, which were significantly lower than those in the distal 2 parts.
Conclusion: In the Latarjet procedure, the proximal-medial part of the coracoid graft demonstrated the most evident stress shielding, which may play an important role in postoperative osteolysis.
Level of evidence: Basic Science Study; Computer Modeling

Keywords: Latarjet procedure; CT-based finite element method; coracoid graft; stress shielding

The Latarjet procedure has been widely used as one of the most reliable surgical options for recurrent anterior shoulder dislocation especially when presenting with a large glenoid bone defect.[4,14,20,22,29,30] Although multiple technical modifications have been reported, the primary concept of this procedure is the transfer of the coracoid

This study was approved by the Institutional Ethical Committee of Sendai City Hospital (SENBYOSO-354).

*Reprint requests: Hirotaka Sano, MD, PhD, Division of Orthopedics, Sendai City Hospital, 1-1-1, Asuto-Nagamachi, Taihaku-ku, Sendai 982-8502, Japan.
E-mail address: sanohirotaka@gmail.com (H. Sano).

1058-2746/$ - see front matter
https://doi.org/10.1016/j.jse.2020.03.037

process with the conjoint tendon to the anterior glenoid rim in the lying position. It is known that there are 3 stabilization mechanisms in this procedure: the sling effect is created by the intersection of the conjoint and inferior subscapularis tendons, the bone effect occurs by the use of the coracoid graft, and the ligament effect occurs through the reattachment of the coracoacromial ligament stump.[8,14,19,31] These mechanisms are able to restore the stability and function of the shoulder joint in more than 95% of patients with significant bone defects.[4] However, several major complications have been reported after this procedure including the osteolysis of the grafted coracoid.[5,7,11,15,36]

In the orthopedic field, it is believed that the pathomechanism of postoperative osteolysis after arthroplasties can be explained by Wolff's law.[27,33] Briefly, the inserted implant causes stress shielding, which leads to the osteolysis of the local bone. Although stress shielding appears to play a crucial role in the pathogenesis of coracoid graft osteolysis after the Latarjet procedure, no biomechanical studies have been conducted to investigate the stress distribution in the coracoid graft.

A computed tomography (CT)-based 3-dimensional (3D) finite element (FE) method has been widely used for investigating the stress distribution within the individual bone to assess the risk of postoperative osteolysis.[27,28] The developed 3D FE model precisely reflects the individual bony architecture, which can visualize the stress distribution inside the bone. In the present study, we attempted to clarify the stress distribution pattern in the coracoid graft after the Latarjet procedure with this method to investigate the risk of the postoperative osteolysis of the coracoid graft. We hypothesized that the proximal-medial part of the coracoid graft would demonstrate the most evident stress shielding, because the previous authors reported that osteolysis was seen most frequently in this part.[7,11,15]

Materials and methods

Development of the FE shoulder model with an anterior glenoid defect (Defect model)

Ten patients with unilateral anterior shoulder instability (9 males and 1 female, age: 17-49 years) were recruited for the present study with written informed consent. CT-DICOM data of the contralateral healthy shoulder in each patient were used for the present study. 3D FE models of the glenohumeral joint were developed using the software Mechanical Finder (version 9.0, Extended Edition; RCCM, Tokyo, Japan). In this software, human bone models can be developed from the CT-DICOM data and a virtual biomechanical testing can be done with these models. To reduce the size of the model, the medial aspect of the scapular body, distal part of the humerus, and the clavicle were excluded from the model. A 25% bony defect was created on the anterior glenoid rim (Defect model). The osteotomy line was set parallel to the longitudinal axis of the glenoid according to the previous biomechanical study.[34] In the software, Mechanical Finder, Young's modulus for both cortical and cancellous bone can be calculated by the Hounsfield unit values.

The distal part of the coracoid process (length: 2.5 cm) was resected for simulating the coracoid osteotomy in the Latarjet procedure. The data of the resected coracoid process were saved as a stereolithography (STL) file for future transfer.

Modeling of the articular cartilage

Articular cartilage was modeled to cover both glenoid and humeral head surfaces to recreate their contact on the FE model. On the basis of the previous report, the cartilage thickness was determined to be 2.0 mm for both the glenoid and humeral head.[25,37] First, the scapular neck of the Defect model was osteotomized, and the glenoid bone was saved in the STL format. After importing the glenoid bone back to the Defect model, the superimposed glenoid bone was moved 2 mm laterally. With this procedure, a 2-mm-thick articular cartilage layer was recreated, which had a completely identical surface geometry to that of the original glenoid bone. However, it should be noted that the recreated cartilage layer did not reflect their precise anatomies. Moreover, the repaired labrum in the Latarjet procedure was not modeled in the present study because of the lack of the information concerning its precise geometry.

Next, the anatomical neck of the humerus was osteotomized and the humeral head was saved as an STL file, which was imported back again to the Defect model. For recreating a 2-mm-thick articular cartilage layer of the humeral head, the superimposed humeral head was magnified by 1.05 diameters to obtain a surface geometry of the articular cartilage that covers the original humeral head. Next, the lateral edge of the magnified articular cartilage layer was manually scraped to constitute a smooth continuity from the cartilage layer to the original bony contour of the anatomical neck for improving the shape of developed models.

Simulation of coracoid transfer

The resected coracoid was imported back to the Defect model. The undersurface of the coracoid graft was made flat and placed on the anterior glenoid defect, which was then rotated around the *x*-, *y*-, and *z*-axes to simulate the Latarjet procedure. The position of the coracoid graft is believed to be one of the most important factors to achieve satisfactory results in the Latarjet procedure. In the present study, care was taken that the coracoid process was placed flush with the glenoid cartilage. Two half-threaded screws (diameter: 3.5 mm, length: 35 mm) were used to fix the grafted coracoid on the glenoid neck. The geometric information for the screws was downloaded from the website https://www.traceparts.com/en. Note that the soft tissues including the capsule, coracoacromial ligament, and conjoint tendon were not modeled in the present study, which means that the coracoid was placed on the anterior glenoid rim as an intra-articular graft.

Arm position

The original FE models were developed at the hanging arm position in neutral rotation, because the CT scan was taken in this position for all cases. For clarifying the role of the arm position in

the intra-articular stress distribution pattern, we attempted to simulate not only the hanging arm position but also the 90° shoulder abducted position according to the previous biomechanical studies.[2,21] For abducting the shoulder joint, the center point of the humeral head was determined to be the rotation center in each FE model. Then, it was abducted around this point in the scapular plane. The abduction angles of the scapula and the humerus were 30° and 60°, respectively (Fig. 1).

Contact conditions

In the Latarjet procedure, the humeral head cartilage may contact not only the glenoid cartilage but also the grafted coracoid process. To standardize the site of contact in the present study, the humeral head was translated 1-2 mm anteroinferiorly in some models so that it contacts both the glenoid cartilage and the grafted coracoid simultaneously. No soft tissue was placed on the grafted coracoid in the present analysis. Instead, gap elements were inserted between the cartilage of the glenoid and that of the humeral head as well as the grafted coracoid. Briefly, inserting gap elements between 2 materials is a simple and easy option to handle their contact. They act like frictionless springs to avoid the invagination of the humeral head to the glenoid or grafted coracoid during the analysis. gap elements were also inserted between the grafted coracoid and the glenoid bone, because the present models were developed from the contralateral normal shoulder. In other words, the present models simulate the early postoperative stage when bony union has not been started yet rather than the stage when the remodeling of the coracoid graft has completed.

Material properties

Young's moduli of the humerus and the scapula were calculated using their CT numbers, on the basis of the data proposed by Keyak et al.[16] Poisson's ratio was determined on the basis of the bone mass density, which was calculated on the basis of the CT data.[18] As for the articular cartilage, both Young's modulus and Poisson's ratio were hypothesized to be 35.0 MPa and 0.49, respectively.[23,24,26] Because the material of half-threaded screws used for the fixation of the coracoid process to the glenoid was hypothesized as titanium alloy, their Young's modulus and Poisson's ratio were determined to be 113.8 GPa and 0.30, respectively. These data were chosen from the database of the software.

Boundary conditions

In the present study, the medial margin of the scapula was completely constrained in all directions. For simplifying the analysis condition and shortening the analysis time, we did not simulate the activity of each muscle. Instead, a standard compressive load (50 N) was applied to the lateral wall of the greater tuberosity toward the center of the glenoid[9,10,34] because we assumed that cuff muscles had some activities even in the postoperative immobilization period. A tensile force (20 N) was applied to the distal portion of the coracoid along the direction of the conjoint tendon in the present study (Fig. 1). No loads were applied to the inserted screws in the present study because we did not have proper information concerning the sites of force application as well as their amounts.

Analysis and data interpretation

Elastic analysis was performed, and the distribution patterns of the Drucker-Prager equivalent stress were investigated to compare the total amount of generated stress in the coracoid graft. The distribution patterns of maximum principal stress in the coracoid graft were visualized as well to compare the amount of tensile stress in each model. Next, to further localize the site with the most evident stress shielding, the coracoid graft was divided into 4 parts (proximal/distal and medial/lateral) (Fig. 2). The mean values of the equivalent stress and the maximum principal stress in each part were compared among 4 parts for determining which part demonstrated the lowest stress in the coracoid graft.

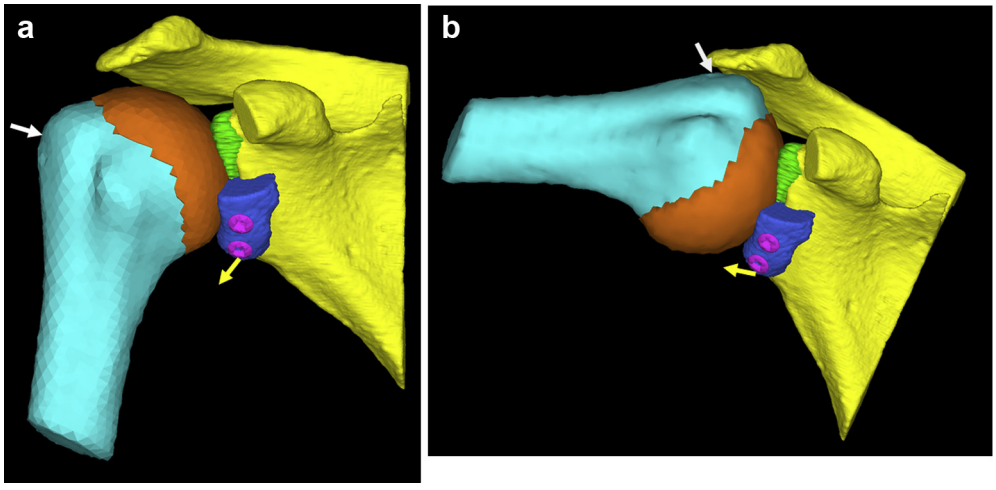

Figure 1 Developed Latarjet models: (**a**) hanging arm position and (**b**) 90° abducted position. The medial border of the scapula is completely constrained. A compressive load (50 N) is applied to the lateral wall of the greater tuberosity toward the center of the glenoid (white arrows). A tensile force (20 N) is applied to the distal portion of the coracoid along the direction of the conjoint tendon (yellow arrows).

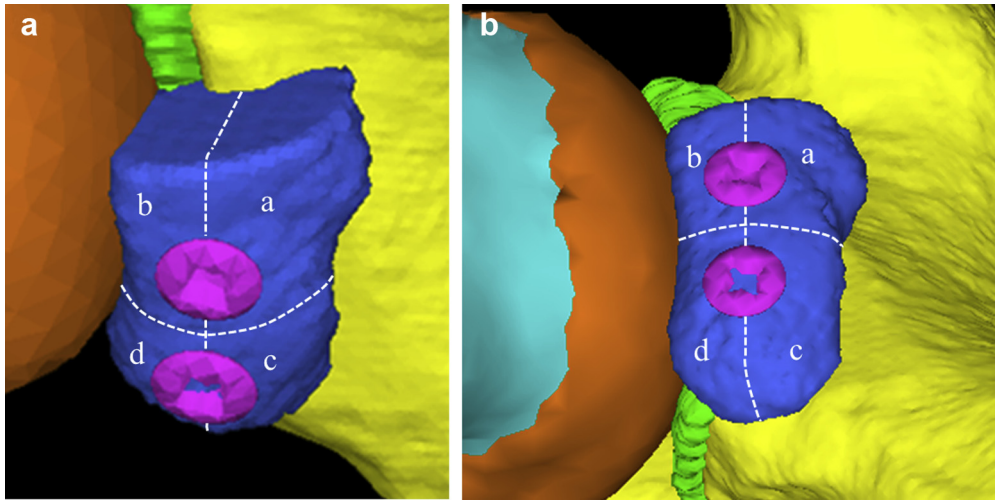

Figure 2 Division of the coracoid graft: (**a**) anterosuperior view and (**b**) anteroinferior view. The coracoid graft is divided into 4 parts (a: proximal-medial part, b: proximal-lateral part, c: distal-medial part, d: distal-lateral part).

Statistical analyses

Repeated measures 1-way analysis of variance followed by Dunnett's multiple comparisons test was used for the comparison of the mean equivalent stress as well as the mean maximum principal stress among the 4 parts of the coracoid graft. A *P*-value of less than .05 was considered to be statistically significant.

Results

Both the equivalent stress and the maximum principal stress demonstrated a similar distribution pattern in the coracoid graft. The proximal half represented a lower stress concentration than the distal half for both arm positions (Figs. 3 and 4). A higher stress concentration was observed in the lateral edge of the coracoid graft than in the medial edge, particularly in the 90° abduction models (Fig. 4).

Among the 4 parts of the coracoid graft, the proximal-medial part showed the lowest stress for both arm positions. The results of the multiple comparisons revealed that the proximal-medial part demonstrated a significantly lower equivalent stress as well as the maximum principal stress than the distal parts for both arm positions. The *P*-values for each comparison were as shown in Figs. 5 and 6. It was interesting to note that a significant difference was also observed between the distal-medial part and the distal-lateral part for both stresses in the 90° abducted position (equivalent stress: $P = .016$, maximum principal stress: $P = .00040$).

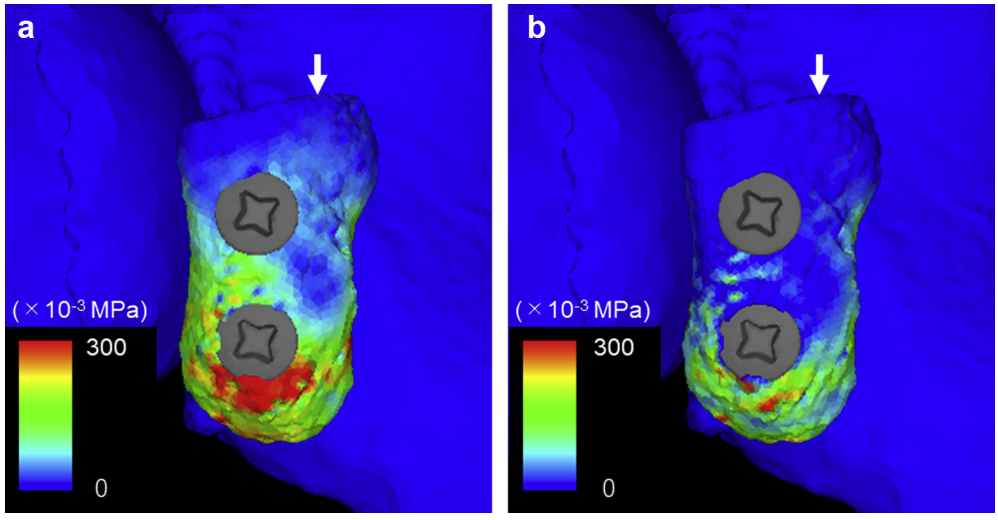

Figure 3 Stress distribution pattern within the coracoid graft in the hanging arm position: (**a**) equivalent stress and (**b**) maximum principal stress. A marked reduction of stress is observed in the proximal half of the coracoid graft (white arrows). Note that only the stress distribution in the coracoid graft is shown.

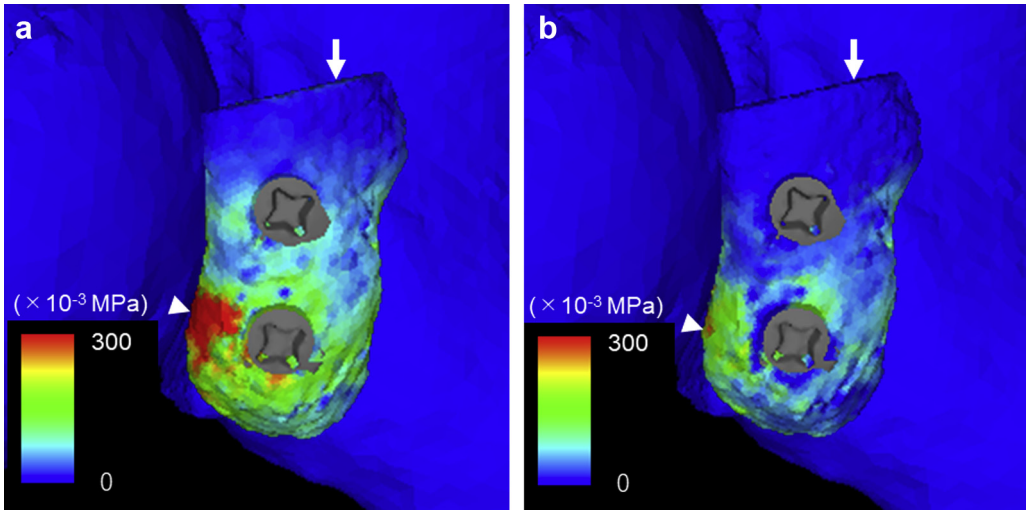

Figure 4 Stress distribution pattern within the coracoid graft in the 90° abducted position: (**a**) equivalent stress and (**b**) maximum principal stress. A reduction of stress is observed in the proximal half in this arm position as well (arrow). On the other hand, a high concentration of the maximum principal stress is observed in its distal-lateral part of the coracoid graft (arrow heads). Note that only the stress distribution in the coracoid graft is shown.

Discussion

This was the first study using a CT-based 3D FE method that focused on the intra-articular stress distribution after the Latarjet procedure. The most important finding of the present study was that the proximal-medial part of the coracoid graft demonstrated the lowest equivalent stress as well as the maximum principal stress among the 4 parts of the coracoid graft.

In the present study, a number of assumptions had to be made during the modeling process. Among them, one of the most challenging steps was the contact conditions between the humeral head and the coracoid graft including the position of the coracoid graft and the soft tissue interposition. As for the position of the coracoid graft, most previous authors recommended fixing the coracoid graft flush or slightly medial to the cartilage surface to reconstruct the glenoid cavity.[1,3,4,6,14,15,17,19,20,31,35] The coracoid placed too far laterally can potentially lead to humeral head abutment, whereas a position of the coracoid 1 cm or more medial to the rim can mean more recurrences.[12,29] In particular, Allain et al[1] described that overly lateral placement of the coracoid graft appeared to lead to symptomatic postoperative glenohumeral osteoarthrosis. De Beer and

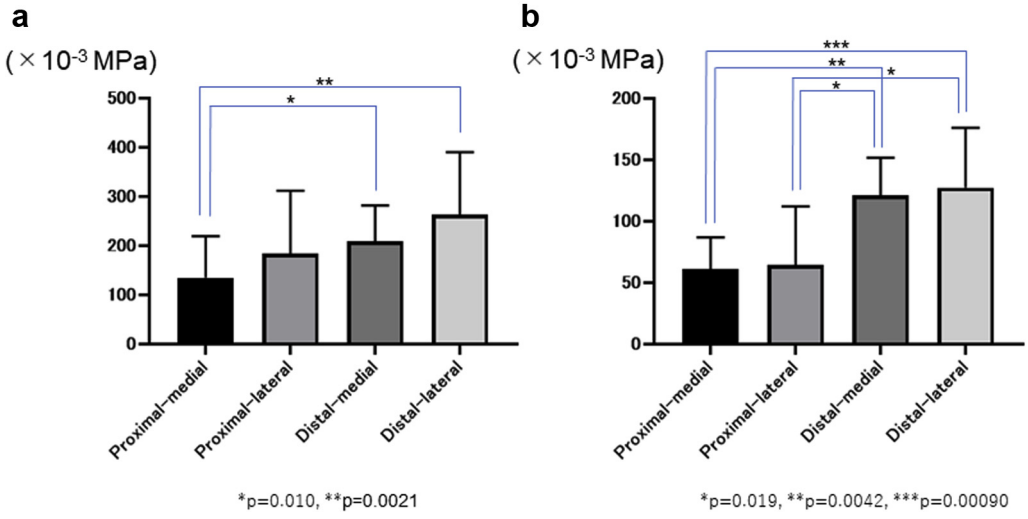

Figure 5 Mean and standard deviation of the equivalent stress (**a**) as well as the maximum principal stress (**b**) within each part of the coracoid graft in the hanging arm position. The proximal-medial part demonstrates the lowest values both for the equivalent stress and the maximum principal stress among the 4 parts in the coracoid graft. Note that a significant difference is observed between the proximal-medial part and the distal-medial and -lateral parts.

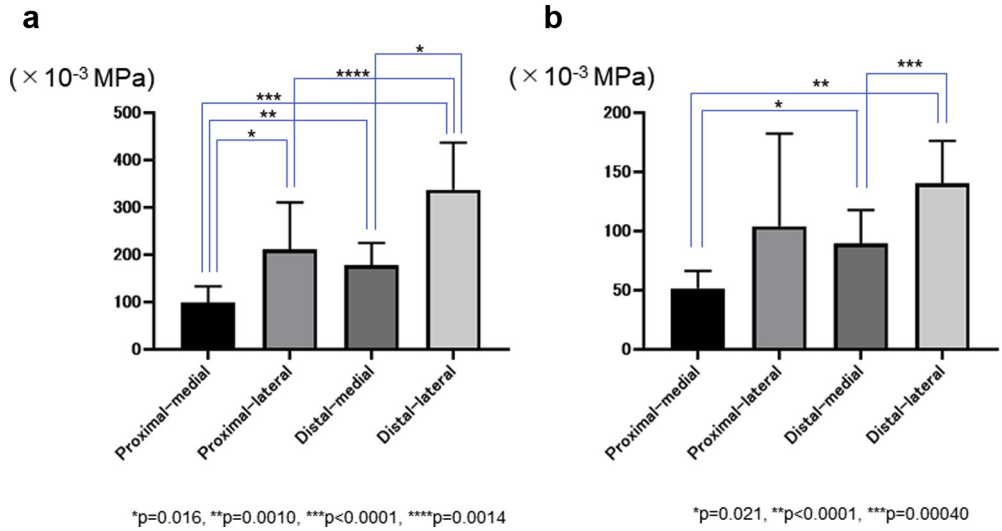

Figure 6 Mean and standard deviation of the equivalent stress (**a**) as well as the maximum principal stress (**b**) within each part of the coracoid graft in the 90° abduction position. The proximal-medial part demonstrates the lowest values for both the equivalent stress and the maximum principal stress among the 4 parts in the coracoid graft. A significant difference is seen between the proximal-medial part and distal 2 parts. Note that there is a significant difference between the distal-medial part and the distal-lateral part for both stresses in this arm position.

Roberts[6] also believed that coracoid grafts placed in a proud position not only increase the peak contact forces anteroinferiorly but also increase the posterosuperior glenoid pressure, indicating a shift posteriorly. They also believed that coracoid grafts placed medially result in increased pressures with high edge loading.[6] On the basis of these reports, we placed the coracoid graft flush with the glenoid cartilage to extend its surface in the present study. The other option was the interposition of the capsule between the humeral head and the coracoid graft. Burkhart et al[4] preferred to repair the capsule to the native glenoid by means of suture anchors, which made the coracoid graft an extra-articular structure, and preventing its articulation directly with the humeral head. Bouju et al[3] also reported that the strictly extracapsular situation of the bone block appeared as an important factor in limiting long-term osteoarthritis. They believed that the capsule reinsertion alleviated the radiologic complications.[3] Biomechanically, the interposition of the capsule between the humeral head and the coracoid graft may reduce the contact pressure that was applied to the coracoid graft. However, for recreating such a condition in the FE analysis, it was necessary to define both the material properties of the inserted capsule and the friction coefficients between the inserted capsule and the humeral head cartilage as well as the inserted capsule and the coracoid graft. Because none of these data were currently available, it may reduce the reliability of the analysis results. Thus, we did not interpose the capsular tissue between the humeral head and the coracoid graft in the present analysis both to simplify the model and to improve the reliability of analysis results. Instead, we adjusted the position of the humeral head to contact both the coracoid graft and the humeral head cartilage, which made it possible to show the mechanical effects of the contact in a simple static analysis.

Previous authors hypothesized the tension of the conjoint tendon to be 2.5-10 N based on the data of the physiological cross-sectional area.[2,8,13,32,34] However, it was impossible to perfectly simulate the physiological tension inherent in the conjoined tendon.[8] In the clinical setting, it seemed that patients tended to move their elbow rather than shoulder for their daily living because their shoulder was immobilized during the early postoperative period. Thus, we applied a tensile load (20 N) to the distal portion of the grafted coracoid to enhance the biomechanical effect of the conjoint tendon inside the coracoid graft in the static analysis.

Regarding the contact between the coracoid graft and the glenoid neck, 2 screws were inserted for the fixation of the coracoid graft onto the anterior glenoid neck in the present study. Because gap elements were inserted between the coracoid graft and the anterior glenoid neck, these 2 bones attached only with the inserted screws. It is known that osteolysis continues even after completion of bony union. As a result, the shape of the coracoid graft might be altered gradually not only by the stress shielding but also by the new bone formation. Because we used CT data of the contralateral healthy shoulders for the development of the Latarjet models, such alteration of the graft shape was not taken into consideration. Therefore, we decided to simulate the situation immediately after surgery before starting bony union.

The Latarjet procedure can alter the intra-articular stress distribution dramatically because it is a nonanatomical

surgical procedure. In the present study, we found that the stress distribution pattern in the coracoid graft well reflected the following factors: the tensile force by the conjoint tendon, the insertion of 2 screws, and the compressive forces by the humeral head as well as the glenoid neck. First, a high stress concentration was observed in the distal parts of the coracoid graft. Such a high stress concentration was caused by the tensile force by the conjoint tendon. On the contrary, the proximal half of the coracoid graft showed a reduction of both the equivalent stress and the maximum principal stress than the distal half for both arm positions. We assumed that the insertion of 2 screws shielded the proximal half of the coracoid from the tensile force of the conjoint tendon. Second, a high stress concentration in the lateral aspects occurred, especially for 90° abducted positions. We assumed that this stress concentration was caused by the contact with the humeral head.

The comparison among the 4 parts of the coracoid graft revealed that the proximal-medial part represented the lowest equivalent as well as the maximum principal stress for both arm positions. Statistical significance was determined between the proximal-medial part and the distal-medial and -lateral parts. It appeared that the stress shielding was most evident in this part because neither the tensile load by the conjoint tendon nor the compressive loads were applied. On the basis of these results, we believed that this part of the coracoid graft had the highest risk of osteolysis.

Reportedly, osteolysis has been more evident in the proximal half than in the distal half.[7,11,36] Di Giacomo et al[7] further localized the site of osteolysis within the grafted coracoid. They found that the superficial part of the proximal coracoid represented the most relevant osteolysis, whereas the distal-deep part was the least involved in osteolysis.[7] These findings were consistent with the results of the current FE analysis. We assumed that the remodeling of the coracoid graft was mainly determined by Wolff's law.[11] Because of the stress shielding, osteolysis might start from the proximal-medial part of the coracoid graft. On the other hand, the lateral parts of the coracoid graft may not be involved by osteolysis, because they were exposed to the compressive force due to the contact with the humeral head. Consequently, the glenoid may eventually be remodeled to its original pear shape, as Kee et al reported.[15]

There were several limitations of the present study. First, the number of samples was rather small. However, all 10 models demonstrated a similar stress distribution pattern for both arm positions. Second, a number of assumptions were made during the modeling process including the loading and contact conditions. Although we could reproduce the glenohumeral joint contact as well as the traction by the conjoint tendon in the present model, the compressive load applied to the inserted screws could not be taken into considerations by the technical reasons. Third, this was a pure simulation study. A future validation study is warranted for confirming the results of the present analysis. However, it would be extremely challenging to measure the precise stress distribution pattern inside the coracoid graft using either cadaveric specimens or living patients. Because the results of the present study were consistent with the previously reported clinical findings, we believed that our models recreated precisely the biomechanical conditions after the Latarjet procedure. In other words, the results of the present study explained what was happening in the coracoid graft after this procedure. Lastly, this was only a static analysis that simulates the condition immediately after surgery. Future studies including the dynamic analysis will be necessary to explain the true intra-articular stress distribution after the Latarjet procedure.

Conclusion

The proximal-medial part of the coracoid graft demonstrated the most evident stress shielding, which may eventually lead to osteolysis. These results are important for shoulder surgeons to understand the pathomechanism of coracoid graft osteolysis after the Latarjet procedure.

Disclaimer

The authors, their immediate families, and any research foundations with which they are affiliated have not received any financial payments or other benefits from any commercial entity related to the subject of this article.

References

1. Allain J, Goutallier D, Glorion C. Long-term results of the Latarjet procedure for the treatment of anterior instability of the shoulder. J Bone Joint Surg Am 1998;80:841-52.
2. Boons HW, Giles JW, Elkinson I, Johnson JA, Athwal GS. Classic versus congruent coracoid positioning during the Latarjet procedure: an in vitro biomechanical comparison. Arthroscopy 2013;29:309-16. https://doi.org/10.1016/j.arthro.2012.09.007
3. Bouju Y, Gadea F, Stanovici J, Moubarak H, Favard L. Shoulder stabilization by modified Latarjet-Patte procedure: results at a minimum 10 years' follow-up, and role in the prevention of osteoarthritis. Orthop Traumatol Surg Res 2014;100:S213-8. https://doi.org/10.1016/j.otsr.2014.03.010
4. Burkhart SS, De Beer JF, Barth JR, Cresswell T, Roberts C, Richards DP. Results of modified Latarjet reconstruction in patients with anteroinferior instability and significant bone loss. Arthroscopy 2007;23:1033-41. https://doi.org/10.1016/j.arthro.2007.08.009
5. Butt U, Charalambous CP. Complications associated with open coracoid transfer procedures for shoulder instability. J Shoulder Elbow Surg 2012;21:1110-9. https://doi.org/10.1016/j.jse.2012.02.008
6. de Beer JF, Roberts C. Glenoid bone defects—open Latarjet with congruent arc modification. Orthop Clin North Am 2010;41:407-15. https://doi.org/10.1016/j.ocl.2010.02.008

7. Di Giacomo G, Costantini A, de Gasperis N, De Vita A, Lin BK, Francone M, et al. Coracoid graft osteolysis after the Latarjet procedure for anteroinferior shoulder instability: a computed tomography scan study of twenty-six patients. J Shoulder Elbow Surg 2011;20:989-95. https://doi.org/10.1016/j.jse.2010.11.016
8. Dines JS, Dodson CC, McGarry MH, Oh JH, Altchek DW, Lee TQ. Contribution of osseous and muscular stabilizing effects with the Latarjet procedure for anterior instability without glenoid bone loss. J Shoulder Elbow Surg 2013;22:1689-94. https://doi.org/10.1016/j.jse.2013.02.014
9. Giles JW, Puskas G, Welsh M, Johnson JA, Athwal GS. Do the traditional and modified Latarjet techniques produce equivalent reconstruction stability and strength? Am J Sports Med 2012;40:2801-7. https://doi.org/10.1177/0363546512460835
10. Gottschalk LJ, Walia P, Patel RM, Kuklis M, Jones MH, Fening SD, et al. Stability of the glenohumeral joint with combined humeral head and glenoid defects: a cadaveric study. Am J Sports Med 2016;44:933-40. https://doi.org/10.1177/0363546515624914
11. Haeni DL, Opsomer G, Sood A, Munji J, Sanchez M, Villain B, et al. Three-dimensional volume measurement of coracoid graft osteolysis after arthroscopic Latarjet procedure. J Shoulder Elbow Surg 2017;26:484-9. https://doi.org/10.1016/j.jse.2016.08.007
12. Hovelius L, Sandstrom B, Olofsson A, Svensson O, Rahme H. The effect of capsular repair, bone block healing, and position on the results of the Bristow-Latarjet procedure (study III): long-term follow-up in 319 shoulders. J Shoulder Elbow Surg 2012;21:647-60. https://doi.org/10.1016/j.jse.2011.03.020
13. Itoigawa Y, Hooke AW, Sperling JW, Steinmann SP, Zhao KD, Yamamoto N, et al. Repairing the capsule to the transferred coracoid preserves external rotation in the modified Latarjet procedure. J Bone Joint Surg Am 2016;98:1484-9. https://doi.org/10.2106/JBJS.15.01069
14. Joshi MA, Young AA, Balestro JC, Walch G. The Latarjet-Patte procedure for recurrent anterior shoulder instability in contact athletes. Orthop Clin North Am 2015;46:105-11. https://doi.org/10.1016/j.ocl.2014.09.005
15. Kee YM, Kim JY, Kim HJ, Sinha S, Rhee YG. Fate of coracoid grafts after the Latarjet procedure: will be analogous to the original glenoid by remodelling. Knee Surg Sports Traumatol Arthrosc 2018;26:926-32. https://doi.org/10.1007/s00167-017-4808-z
16. Keyak JH, Rossi SA, Jones KA, Skinner HB. Prediction of femoral fracture load using automated finite element modeling. J Biomech 1998;31:125-33.
17. Lafosse L, Lejeune E, Bouchard A, Kakuda C, Gobezie R, Kochhar T. The arthroscopic Latarjet procedure for the treatment of anterior shoulder instability. Arthroscopy 2007;23. https://doi.org/10.1016/j.arthro.2007.06.008. 1242.e1241-5.
18. Minamisawa I. A biomechanical study on the senile intracapsular fracture of the femoral neck—speculation concerning the fracture lines and etiological factors. J Jpn Orthop Assoc 1981;55:167-81.
19. Mizuno N, Denard PJ, Raiss P, Melis B, Walch G. Long-term results of the Latarjet procedure for anterior instability of the shoulder. J Shoulder Elbow Surg 2014;23:1691-9. https://doi.org/10.1016/j.jse.2014.02.015
20. Neyton L, Young A, Dawidziak B, Visona E, Hager JP, Fournier Y, et al. Surgical treatment of anterior instability in rugby union players: clinical and radiographic results of the Latarjet-Patte procedure with minimum 5-year follow-up. J Shoulder Elbow Surg 2012;21:1721-7. https://doi.org/10.1016/j.jse.2012.01.023
21. Nourissat G, Delaroche C, Bouillet B, Doursounian L, Aim F. Optimization of bone-block positioning in the Bristow-Latarjet procedure: a biomechanical study. Orthop Traumatol Surg Res 2014;100:509-13. https://doi.org/10.1016/j.otsr.2014.03.023
22. Ranalletta M, Rossi LA, Bertona A, Tanoira I, Maignon GD, Bongiovanni SL. Modified Latarjet procedure without capsulolabral repair for the treatment of failed previous operative stabilizations in athletes. Arthroscopy 2018;34:1421-7. https://doi.org/10.1016/j.arthro.2017.12.006
23. Sano H, Hatta T, Yamamoto N, Itoi E. Stress distribution within rotator cuff tendons with a crescent-shaped and an L-shaped tear. Am J Sports Med 2013;41:2262-9. https://doi.org/10.1177/0363546513497565
24. Sano H, Tokunaga M, Noguchi M, Inawashiro T, Irie T, Abe H, et al. Tight medial knot tying may increase retearing risk after transosseous equivalent repair of rotator cuff tendon. Biomed Mater Eng 2017;28:267-77. https://doi.org/10.3233/BME-171673
25. Schleich C, Bittersohl B, Antoch G, Krauspe R, Zilkens C, Kircher J. Thickness distribution of glenohumeral joint cartilage. Cartilage 2017;8:105-11. https://doi.org/10.1177/1947603516651669
26. Seki N, Itoi E, Shibuya Y, Wakabayashi I, Sano H, Sashi R, et al. Mechanical environment of the supraspinatus tendon: three-dimensional finite element model analysis. J Orthop Sci 2008;13:348-53. https://doi.org/10.1007/s00776-008-1240-8
27. Sumner DR. Long-term implant fixation and stress-shielding in total hip replacement. J Biomech 2015;48:797-800. https://doi.org/10.1016/j.jbiomech.2014.12.021
28. Thompson SM, Yohuno D, Bradley WN, Crocombe AD. Finite element analysis: a comparison of an all-polyethylene tibial implant and its metal-backed equivalent. Knee Surg Sports Traumatol Arthrosc 2016;24:2560-6. https://doi.org/10.1007/s00167-015-3923-y
29. van der Linde JA, Wessel RN, Trantalis JN, van den Bekerom M. The Classic Review of Latarjet (1954) on the treatment of recurrent shoulder dislocations. J ISAKOS 2018;3:242-8. https://doi.org/10.1136/jisakos-2017-000153
30. Walch G. Chronic anterior glenohumeral instability. J Bone Joint Surg Br 1996;78:670-7.
31. Walch GB P. Latarjet-Bristow procedure for recurrent anterior instability. Tech Shoulder Elbow Surg 2000;1:256-61.
32. Wellmann M, Petersen W, Zantop T, Herbort M, Kobbe P, Raschke MJ, et al. Open shoulder repair of osseous glenoid defects: biomechanical effectiveness of the Latarjet procedure versus a contoured structural bone graft. Am J Sports Med 2009;37:87-94. https://doi.org/10.1177/0363546508326714
33. Yamada H, Yoshihara Y, Henmi O, Morita M, Shiromoto Y, Kawano T, et al. Cementless total hip replacement: past, present, and future. J Orthop Sci 2009;14:228-41. https://doi.org/10.1007/s00776-008-1317-4
34. Yamamoto N, Muraki T, An KN, Sperling JW, Cofield RH, Itoi E, et al. The stabilizing mechanism of the Latarjet procedure: a cadaveric study. J Bone Joint Surg Am 2013;95:1390-7. https://doi.org/10.2106/JBJS.L.00777
35. Young AA, Maia R, Berhouet J, Walch G. Open Latarjet procedure for management of bone loss in anterior instability of the glenohumeral joint. J Shoulder Elbow Surg 2011;20:S61-9. https://doi.org/10.1016/j.jse.2010.07.022
36. Zhu YM, Jiang CY, Lu Y, Li FL, Wu G. Coracoid bone graft resorption after Latarjet procedure is underestimated: a new classification system and a clinical review with computed tomography evaluation. J Shoulder Elbow Surg 2015;24:1782-8. https://doi.org/10.1016/j.jse.2015.05.039
37. Zumstein V, Kraljevic M, Conzen A, Hoechel S, Muller-Gerbl M. Thickness distribution of the glenohumeral joint cartilage: a quantitative study using computed tomography. Surg Radiol Anat 2014;36:327-31. https://doi.org/10.1007/s00276-013-1221-2